PETROLOGIC CONTEXT OF PHOSPHATE MINERALS IN APOLLO 14 SAMPLES. Hannah C. O'Brien*[1], Katharine L. Robinson[2], and David A. Kring[2]. [1]Civil, Environmental Engineering and Earth Science Department, University of Notre Dame,156 Fitzpatrick Hall Notre Dame, IN 46556. [2]Lunar and Planetary Institute, USRA, 3600 Bay Area Blvd., Houston, TX 77058. (hobrien5@nd.edu).

Introduction: Recognition of water in the lunar interior [1-5] has provided a new tool for probing magmatic processes in the lunar interior. Thus far, water and H isotopes have been measured in lunar glasses, melt inclusions, and apatite ($Ca_5(PO_4)_3$[F, Cl, OH]) [1-4]. Previous examination of lunar apatite in ancient highland samples (**Fig. 1**), suggested a correlation between age and δD [3]. An independent set of apatite in ~4.3 Ga Apollo 15 quartz monzodiorites (QMD) produced some of the lowest δD values measured thus far in lunar apatite [5] (**Fig. 1**). Interestingly, geochronologic analyses of lunar samples, coupled with numerical modeling, suggest a period of enhanced magmatism circa 4.30-4.36 Ga may have been catalyzed by the impact event that produced the immense South Pole-Aitken (SPA) impact basin [6]. Did this period of enhanced magmatism and the resulting processes tap a unique δD water reservoir or somehow fractionate a δD reservoir to produce the low values?

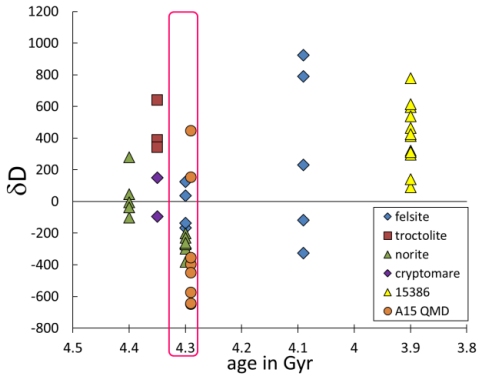

Figure 1: *Plot of apatite δD versus sample age in Ga by rock type, including felsite, troctolite, norite, cryptomare basalt, KREEP basalt 15386, and Apollo 15 QMDs. The ages of several samples with low δD cluster around 4.3 Ga. Data from [3,7,8,14,20-23].*

To begin testing this idea, we examine here two Apollo 14 samples ranging in age from ~4.2 to ~4.36 Ga [8-11], plus a third sample with plausibly a similar age. We identify and petrologically characterized apatite and other phosphate minerals in them in advance of [H_2O], δD, and Cl-isotope analyses. Additionally, we locate U-Pb carriers, such as zircon, that can be used to independently assess the ages of the samples.

Methods: Back-scattered electron imagery and X-ray elemental mapping were conducted at the Johnson Space Center (JSC) with a JEOL 7600 field emission scanning electron microscope to identify phosphate and Zr-bearing minerals within each sample [12](**Fig. 2**).

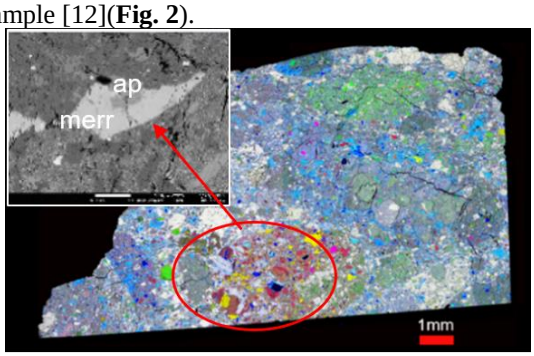

Figure 2: *False color X-ray map of 14306,60, with Al in white, Ca in yellow, Ti in pink, Si in blue, K in cyan, Fe in red, and Mg in green. Phosphate appears bright yellow in the map. The inset is a magnified view of phosphate grain #10, composed of merrillite with an apatite intergrowth.*

Silicate mineral chemistry was measured using a Cameca SX-100 electron microprobe at JSC with a 15 kV, 20 nA beam. For phases susceptible to volatilization, the beam was defocused to 5 to 10 µm and the current reduced to 10 nA. Prior to analysis, the instrument was calibrated for Na, Mg, Al, Si, P, K, Ca, S, Ti, Fe, and Mn using natural and synthetic mineral standards. Phosphate chemistry was determined using a JEOL JXA-8530 electron microprobe. The instrument was calibrated for F, Na, Mg, Si, Ca, S, Ce, Cl, P, Sr, La, and Fe, using well-characterized synthetic and natural mineral standards. Fluorine was measured first to avoid volatilization during analysis. Chlorine and F abundances were measured and OH was calculated based on the apparent vacancy assuming Cl+F+OH = 1 in the halogen (X) site of the apatite [13].

Results and Discussion: We examined three Apollo 14 breccias: 14303,209; 14314,10; and 14306,60. All three samples likely originated from the Fra Mauro Formation (Imbrium ejecta) [14,15].

Sample 14303,209 is a ~7.5 mm felsite ("granite") clast, considered pristine [16], in a crystalline-matrix breccia. The sample is rich in K-feldspar, often intergrown with silica, and plagioclase. Zircon in this clast has an age of 4.308 ±0.3 Ga [8]. Sixteen phosphate crystals were identified in this sample. Of those phosphate crystals, 7 may be suitable for secondary ion mass spectrometry (SIMS) analysis which requires grains at least 5 to 10 µm in width. Apatite in this sample contains 0.3 to 1.3 wt.% Cl and 2.5 to 3.4 wt.% F. As

seen in **Fig. 3**, some of the apatite grains in this sample are compositionally similar those in 14053.

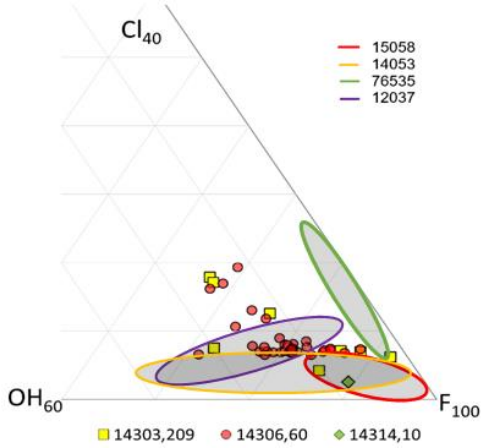

Figure 3: *Truncated apatite ternary of samples investigated. OH is estimated by difference, assuming the X site = OH+Cl+F = 1, and are likely lower than they appear on this plot. Fields are Apollo literature data adapted from [17].*

Sample 14314,10 contains a wide variety of clasts including mare basalt and annealed glass, displays shock features in zoned olivine xenocrysts, and is rich in plagioclase and silica in the interstitial groundmass [18]. The largest phosphate crystals are found within a ~3 mm impact melt breccia clast. This clast is also characterized by sodic plagioclase, ranging from 0.57 to 3.15 wt. % Na_2O, with the highest [Na] present in an Fe-rich region of the clast, where the largest phosphate crystals are found. Eleven phosphate crystals, mostly merrillite with apatite inclusions, were identified in this sample; two of the apatite grains are potentially suitable for SIMS analysis. The largest apatite grains in this sample are inclusions in an ~300 μm merrillite, with significantly lower [Cl] than in apatite measured in our other samples (**Fig. 3**). Apatite in this sample contains ~0.2 wt.% Cl and ~3.4 wt.% F. An age has not yet been obtained for this sample.

Sample 14306,60 is a clast-rich crystalline matrix breccia with large Fe-rich, Si-rich, and magnesian clasts. Apatite and large zircon grains are found in norite fragments that are ~4.2 Ga [9-11]. Phosphate crystals are abundant in this sample, with 18 total identified crystals, including 13 apatite grains potentially suitable for SIMS analysis. As seen in **Fig. 2**, apatite grains suitable for analysis with a size of at least 5 to 10 μm in width are present as an intergrowth or rim on merrillite grains. Phosphate crystals in 14306,60 are concentrated in a large, brecciated, and potentially gabbronorite (GN) clast. However, a high proportion (~19%) of phosphate grains in this clast suggest it may not be representative of its source lithology, as phosphate is not a major mineral in GN. This clast also contains exsolved, Fe-rich pyroxene and zircon and silica intergrowths. One region of the clast is more plagioclase- and Mg-pyroxene-rich and contains fewer phosphate crystals relative to the clast as a whole **(Fig. 2).** The plagioclase An content of this clast is similar to those in other lunar GN: 83 to 96 [19]. However the Mg# in the Fe-rich pyroxene is significantly lower, from 38 to 49 **(Fig. 4)** vs. lunar GN with Mg# 64 to 78 [19]. Apatite found outside the GN clast contains less Cl than apatite within the clast (**Fig. 3**). Apatite in this sample contains 0.3 to 1.4 wt.% Cl and 2.5 to 3.7 wt.% F.

Conclusions: Sample 14303,209 is granitic crystalline matrix breccia with 16 phosphate crystals in K-feldspar- and plagioclase-rich regions. Sample 14314,10 is a crystalline matrix breccia with a large, distinct impact melt breccia clast; 11 phosphate crystals were identified predominantly within the clast and near plagioclase crystals. Sample 14306,60 is a clast-rich crystalline matrix breccia with multiple lithic clasts. Eighteen phosphate grains were identified in this sample, with a concentration of apatite in a large, Fe-rich, potentially GN clast. Collectively, 45 phosphate grains were identified, 22 of which may be suitable for SIMS measurement of [H_2O], δD, and Cl-isotopes. Future analyses of volatiles from these ancient A14 samples may help reveal the nature of volatiles related to magmatism generated by the SPA basin-forming impact.

References: [1] Saal A. E. et al (2013) *Science, 340,* 1317–1320. [2] Hauri E. H. et al. (2015) *EPSL, 409*, 252–264. [3] Barnes J. J. et al. (2014) *EPSL, 390*, 244–252. [4] McCubbin F. M. et al. (2010) *PNAS, 107*, 11223–11228. [5] Robinson K. L. and Taylor G. J. (2014) *Nat. Geosci., 7*, 401–408. [6] Kring D.A. et al. (2015) *Bombardment Workshop III*, Abstract #3009. [7] Robinson K.L. et al., (2016) *GCA, 188*, 244-260. [8] Meyer C. et al. (1996) *MAPS, 31*, 370–387. [9] Compston W. et al. (1984) *LPS XIV*, 182–183. [10] Meyer C. et al. (1991) *LPS XXII*, Abstract #895. [11] Nemchin A. A. et al. (2008) *GCA, 72*, 668–689. [12] Joy K. H. et al. (2012) *Science, 336*, 1426–1429. [13] Boyce J. W. et al. (2010) *Nature, 466*, 466–469. [14] Carlson R. W. et al. (2014) *Philos. Trans. A Math. Phys. Eng. Sci., 372*, 20130246. [15] Swann G. A. et al. (1977) *USGS Prof. Paper 880*. [17] Warren P. H. et al. (1983) *EPSL, 64*, 175–185. [16] Boyce J. W. et al. (2014) *Science, 344*, 400–402. [18] Dence M. R. and Plant A. G. (1972) *Proc. 3rd Lunar Sci. Conf.*, 379–399. [19] Shearer C. K. et al. (2015) *Amer. Min., 100*, 294–325.[20] Tartèse R. et al. (2014) *Geology, 42*, 363–366. [21] Andreasen R. et al. (2013) *LPS XLIV*, Abstract #2887. [22] Borg L. et al. (2013) *LPS XLIV*, Abstract #1563. [23] Terada K. et al. (2007) *Nature, 450*, 849–853.